Characterization of a vacuum-arc discharge in tin vapor using time-resolved plasma imaging and extreme ultraviolet spectrometry

E. R. Kieft,* J. J. A. M. van der Mullen,† and G. M. W. Kroesen
Department of Applied Physics, Eindhoven University of Technology, P.O. Box 513, 5600 MB Eindhoven, The Netherlands

V. Banine
ASML Netherlands B.V., De Run 6501, 5504 DR Veldhoven, The Netherlands

K. N. Koshelev
ISAN, Troitsk, Moscow Region, 142092, Russia
(Received 25 June 2004; published 23 February 2005)

Discharge sources in tin vapor have recently been receiving increased attention as candidate extreme ultraviolet (EUV) light sources for application in semiconductor lithography, because of their favorable spectrum near 13.5 nm. In the ASML EUV laboratory, time-resolved pinhole imaging in the EUV and two-dimensional imaging in visible light have been applied for qualitative characterization of the evolution of a vacuum-arc tin vapor discharge. An EUV spectrometer has been used to find the dominant ionization stages of tin as a function of time during the plasma evolution of the discharge.

DOI: 10.1103/PhysRevE.71.026409 PACS number(s): 52.25.Os, 52.70.Kz, 52.70.La, 52.80.−s

I. INTRODUCTION

Future tools for semiconductor lithography, as currently under development, will apply light in the extreme ultraviolet (EUV) wavelength range for the projection of small-scale patterns onto wafers. Due to the limited reflectivity of the proposed multilayer optics for these wavelengths, and high throughput demands for commercial tools, very powerful EUV light sources are required for this application. Promising candidate sources include various types of discharge plasma sources.

Since the end of 2001, an EUV Laboratory has been in operation at ASML in Veldhoven. One of its aims is the characterization of candidate EUV sources, and their suitability for application in lithography. In the framework of a research cooperation between ASML and TU/e, a hollow cathode discharge in xenon from Philips EUV has been investigated using time-resolved pinhole imaging and EUV spectrometry [1].

Recently, various research groups worldwide have put an increased effort in investigating the replacement of xenon by tin as the working element in EUV discharges (several contributions in [2]). Although it creates some new challenges in the field of debris mitigation, tin has the major advantage over xenon that it has an EUV spectrum that is strongly peaked at the desired wavelength (around 13.5 nm).

A triggered vacuum arc in Sn vapor from the Russian Institute of Spectroscopy (ISAN) has been in operation in the EUV laboratory since March 2003. The discharge region consists of a flat, grounded cathode that is covered with a thin layer of liquid tin, and an anode located about 3 to 3.5 mm above the cathode. The anode has either a round or a semicircular hole in its center; the version with a semicircular hole was used in the experiments presented here. A schematic picture of the electrode cross section is given in Fig. 1. Before the start of the discharge, a positive electrical potential of 4 kV is applied to the anode. The discharge is started by the creation of a cloud of partly ionized tin vapor above the cathode, which expands toward the edges of the anode. Once the plasma near the anode has reached a sufficiently high density, a discharge is started. The current through the discharge increases to almost 20 kA in only a few tens of ns time, and a multiply ionized, EUV emitting plasma is formed. The strong current causes a pinch effect, meaning that due to Lorentz forces acting on the charged particles in the plasma, the plasma is compressed in radial direction to a needlelike shape on the axis of the discharge, with a diameter on the order of 100 μm. In view of the dynamics of the plasma, the time development of the discharge can be roughly split up into four main phases: the trigger plasma, before the discharge current has started (1); the prepinch

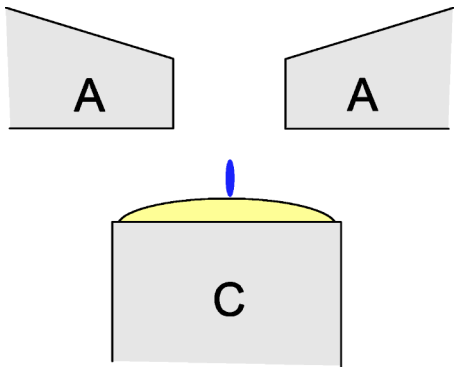

FIG. 1. A schematic cross section of the electrodes of the tin vapor discharge, with at the top the anode (A) with a central hole in it, and the cathode (C) at the bottom. The small, elongated shape in the center represents the position of the pinch plasma.

*Email address: e.r.kieft@tue.nl
†Corresponding author. Email address: j.j.a.m.v.d.mullen@tue.nl

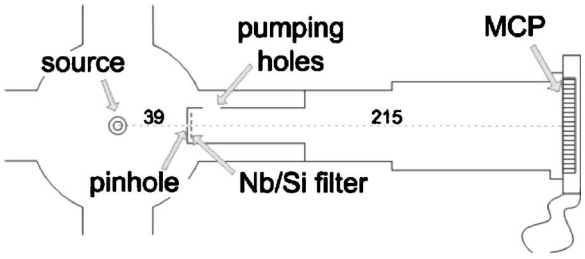

FIG. 2. Schematic view of the pinhole setup for plasma imaging at EUV wavelengths. Pumping holes in the pinhole holder were used for pumping down the space between the pinhole and the MCP. The numbers give the distances between the source, the pinhole and the MCP front surface in mm. The camera that was mounted behind the MCP assembly is not shown here.

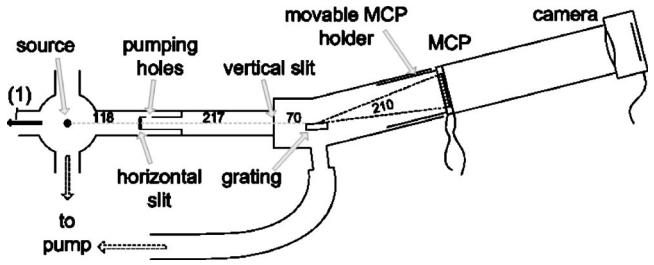

FIG. 3. A schematic top-view image of the setup for EUV spectrometry on the tin discharge. On the left the plasma source is shown in its vacuum chamber. The space between both slits is pumped down through apertures in the first slit holder. The inside of the EUV spectrometer is pumped down through a separate connection to the turbo pump. The arrow marked by (1) indicates the direction where the EUV power meter was mounted. Not all sizes are drawn to scale.

phase, in which the plasma is heated and ionized by the strong electrical current, and starts to compress (2); the pinch itself (3); and a decay phase (4). The actual pinch phase has a duration on the order of 10 ns only, and it is therefore very short-lived compared to the other phases of the discharge. This makes the center of the pinch phase a suitable zero on the time scale when one is describing the properties of the plasma in the other phases. The pinch occurs about 300 ns after the ignition of the discharge. The repetition rate of the source was limited to 5 Hz in the current work.

This article describes a series of experiments, similar in nature to those presented in [1], for the characterization of the tin discharge. Time-resolved pinhole images in the EUV range have been recorded. Time-resolved imaging has also been performed in the visible light, to achieve better understanding for those phases of the discharge in which the plasma is not hot enough to emit EUV radiation. Combined, they can be used to describe the plasma evolution during the entire discharge.

Time-resolved EUV spectrometry, supported by COWAN code calculations [3], serves to determine the dominant ionization stages in the hottest phases of the plasma, and helps

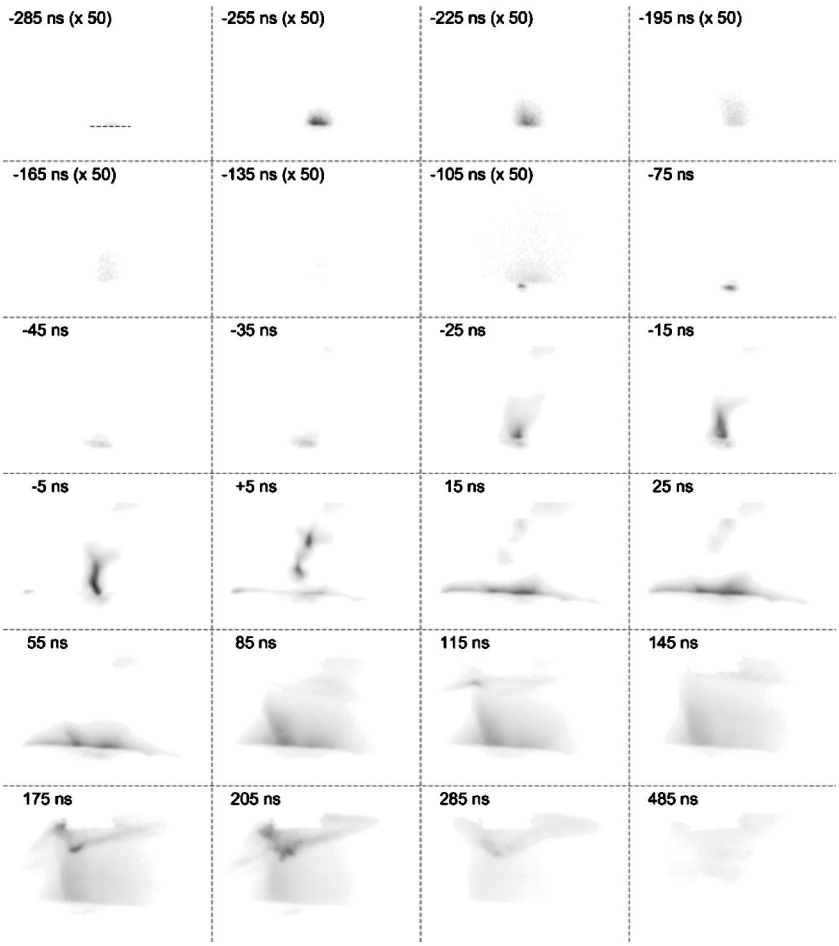

FIG. 4. Time-resolved visible light images recorded during the tin discharge. Each image corresponds to an area in the source of 5.2 mm wide times 3.9 mm high. The horizontal dotted line in the first image indicates the position of the cathode surface and corresponds to a length of 1 mm. The anode is near the top of each image; however, the plasma very close to the anode is obstructed from view by some small structures on the anode between the discharge and the camera. The time indication in the top left corner of each image is relative to the center of the pinch phase. The ignition of the discharge happens at about −300 ns.

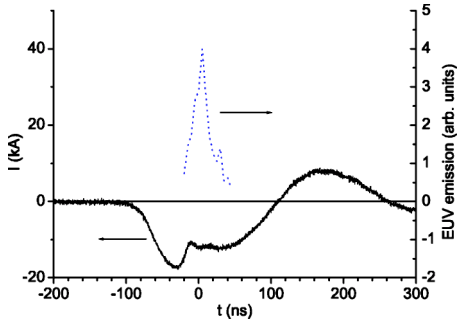

FIG. 5. Discharge current (solid curve) and EUV emission derived from MCP images (dotted curve) during the discharge. The absolute value of the current is derived from the electrical circuit parameters, and is only approximate.

to compare the characteristics of different spatial parts of the discharge.

II. EXPERIMENT

Basic descriptions of the pinhole camera and EUV spectrometer setups have already been given in [1]. In the present case, it was more convenient to use smaller distances between the various parts of the imaging system. Figure 2 shows a schematic view of the pinhole imaging setup. For pinhole imaging, the distance between source and pinhole was reduced to 39 mm, whereas a distance of 215 mm was used for the distance from the pinhole to a multichannel plate (MCP) detector, resulting in a geometrical magnification factor of $M=5.5$. A 150 nm thick silicon/niobium filter was mounted just behind the pinhole to avoid blurring of the image by radiation from wavelengths above about 20 nm. The output light from the MCP was recorded by a commercial-type digital camera. The gain provided by the MCP could be varied by changing the input voltage, to reveal weak features of EUV emission early and late in the pulse, while preventing saturation of the MCP and the camera during the compression and pinch stages.

A schematic picture of the EUV spectrometry setup is shown in Fig. 3. A 1200 l/mm grating with 1 m radius of curvature was used at a 4° grazing angle of incidence for the recording of EUV spectra in the 5–30 nm wavelength range. Spatial resolution, in the vertical dimension of the discharge, was achieved by inserting a horizontally orientated slit into the spectrometry setup in front of the vertical EUV spectrometer entrance slit. Distances between source, first slit, second slit, grating and MCP were 118 mm, 217 mm, 70 mm and 210 mm, respectively. This resulted in a spatial magnification factor of 4.14 on the front surface of the MCP. Both for pinhole imaging and for spectrometry, signals were recorded from a direction perpendicular to the discharge's axis of symmetry.

FIG. 6. A four-times intensified image recorded at 65 ns before the pinch. Visible light emission shows up not far from the anode (near the top of the image).

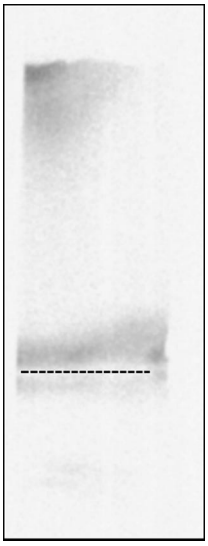

FIG. 7. EUV pinhole image of the discharge at 40 ns before the pinch, recorded at an increased MCP voltage of 6.24 kV. The area of the image corresponds to an area of 1.6 mm wide and 4.2 mm high in the source. The dashed line gives an indication of the position of the surface of the cathode. Like in the visible light images, the real anode position corresponds to the top of the frame, but the region closest to the anode is obstructed from the view. In this image, some EUV emission is visible from the region just outside this obstruction.

A wavelength calibration was achieved by comparing the Sn spectrum with the spectrum from an experiment where the tin cathode was replaced by a cathode that was filled with a mixture containing lithium and magnesium, for which the line wavelengths in the EUV are accurately known (as compiled by [4]). The lines that were used for the calibration were the Mg V $2p^3 3s(2D)^1D_2$–$2P^4(1D)^1D_2$ line and the Mg VI $2s2p^4(3P)^2P_{3/2}$–$2s^2 2p^3(2P)^2D_{5/2}$ line at 14.29 nm [5,6] and 27.04 nm [6], respectively. Both lines were chosen because they are far apart in the spectrum, they were clearly visible above the background and they were well isolated, so that their position could be determined with good accuracy.

For two-dimensional imaging in the visible light range, an intensified charge-coupled device (ICCD) camera from Andor, type DH510-18, was mounted behind a set of two achromatic lenses with 600 mm focal length, arranged to achieve a magnification factor of 1.14. The discharge was imaged into a horizontal direction, perpendicular to the axis of symmetry of the discharge, and through a glass window. The wavelength sensitivity of this imaging system was limited by the transparency of the glass window and lenses, and the sensitivity curve of the camera's photocathode, to about 300–850 nm. To avoid overexposure of the ICCD camera (even at the lowest gain setting of its MCP), an aperture of 3

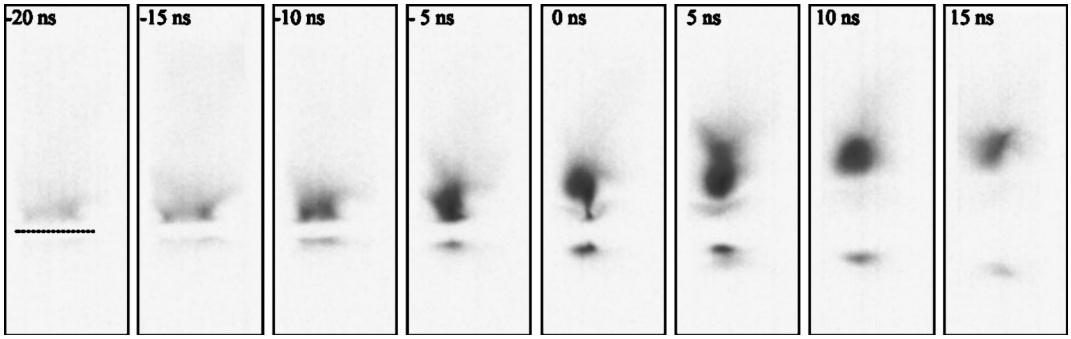

FIG. 8. Series of time-resolved EUV pinhole images during the tin discharge. The images were recorded from 20 ns before until 15 ns after the pinch, in 5 ns time steps. The dotted line in the first image corresponds to a length of 1 mm in the source, and indicates the position of the cathode surface. Each frame corresponds to a size of 1.6×4.2 mm. The feature below this line, near the bottom of each image, is due to a reflection of the plasma EUV emission from the surface of the cathode. The anode is just outside the upper edge of each image.

mm diameter was placed between the two lenses. As in the case of the EUV diagnostics, gating of the imaging system was achieved by switching of a high voltage over the MCP.

The triggering of the diagnostics was in both cases synchronized to the ignition of the discharge. Typically, the time resolution that could be achieved relative to the evolution of the plasma, was on the order of 10 ns, and was limited by both the pulse-to-pulse jitter in the discharge of about 5 ns, and the effective optical gate time of 5 ns.

A magnetic field probe in the electric circuit provided a current signal, displayed on a fast oscilloscope. This signal served as a monitor for the stability of the source. During the EUV experiments, an additional monitor was provided by a voltage signal from a photodiode, that was mounted behind an arrangement of two multilayer mirrors and a silicon/niobium filter. The arrangement was positioned diametrically across the EUV spectrometer, in the horizontal plane of the discharge. This tool provided information about the absolute 'in-band' EUV emission per pulse in a 2% wavelength band around 13.5 nm.

III. PLASMA EVOLUTION

In this section, a detailed, although mainly qualitative, description of the evolution of the discharge as a function of time during the discharge pulse will be given on the basis of a series of visible light and EUV images. The visible light images, which cover the entire time range relevant for the discharge, are shown in Fig. 4. In the plasma imaging experiments, the position where the discharge current attached to the anode was about 3 mm away from the cathode surface. However, the region closest to the anode is obstructed from view by some small structures that are on the anode between the discharge and the camera.

The timing indicated in the top left corner of each image is relative to the pinch, as explained in Sec. I. For the first seven images, the radiation was very weak, so that their intensity had to be digitally increased by a factor 50 relative to the other images. Figure 5 shows typical plots as a function of time of the discharge current and the integrated EUV emission, as derived from the MCP images.

The first six images of Fig. 4 (up to 135 ns before the pinch) only show a weak, decaying plasma that was created by the discharge ignition. What follows is a fast transition to the high-current phase of the discharge, as can be derived from Fig. 5. The first sign of this is the appearance of a bright spot on the cathode, followed by increased emission from a region near the cathode. Also, a spot appears near the anode about 65 ns before the pinch. A four-times intensified image of the visible emission at this time, showing the emission near the anode, is shown in Fig. 6. The emission becomes visible on the intensity scale of Fig. 4 only in the images at -35 and -25 ns.

The anode spot must be generated by a thin, but very hot plasma. This is proven by the fact that it also shows up in the EUV images, as shown in Fig. 7. The image in this figure was recorded 40 ns before the pinch at an MCP voltage of 6.24 kV, and the signal was increased by a factor 4 during digital processing.

Compression of the discharge plasma starts about 30 ns before the actual pinch. During compression, the EUV emission rapidly increases, as is shown in the first four images of Fig. 8. This series of images was recorded between 20 ns before and 15 ns after the pinch at an MCP voltage of 5.25 kV. Effectively, the sensitivity of these recordings was about 30 times lower than in Fig. 7.

The images for 0–15 ns after the pinch show that a ball of plasma moves in the direction away from the cathode, at a velocity of about 4×10^4 m s^{-1}. A similar phenomenon can be observed in the visible light images of Fig. 4. A possible explanation comes from the fact that the current-induced Lorentz force does confine the plasma in the radial, but not in the axial direction. Since the surface of the cathode is close to the bottom of the pinch, the plasma can only escape in the upward axial direction.

Just after the pinch, visible light plasma radiation appears along the cathode surface. Since a similar emission feature does not appear in the EUV, it must be generated by a much cooler plasma. Most likely, the current through the pinch plasma and absorption of EUV radiation lead to heating of the liquid tin on the cathode surface. Evaporation and partial ionization of tin from the cathode can result in a relatively cool plasma.

In the next 150 ns, the "cool" plasma expands and travels toward the anode. About 100 ns after the pinch, a filament-like structure appears near the anode. This structure might be

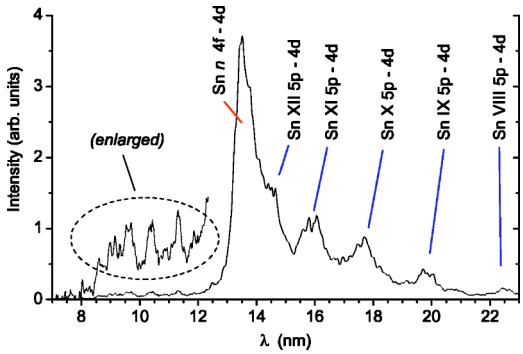

FIG. 9. An example of a recorded EUV spectrum from the tin source, including tentative identifications of the UTAs. This particular spectrum corresponds to the region near the cathode during the pinch phase. The dotted curve is the same spectrum for the lower wavelength part, but on a ten times magnified scale.

created by evaporation of tin from the anode that was deposited there during previous discharge pulses. The intensity of the filament emission increases after 150 ns, perhaps due to a collision with the expanding plasma from the cathode. The anode plasma expands back toward the cathode, but after this time the emission gradually decays. Since these dynamics are not relevant for the EUV emission, we have not studied them in detail.

IV. TIME-RESOLVED EUV SPECTRA

A typical example of the EUV spectrum of the tin source is shown in Fig. 9. The spectrum in this figure corresponds to the emission from near the cathode in the pinch phase, during which the EUV emission is strongest. Calculations using the COWAN computer code [3] reveal that the large peak at 13.5 nm is caused by $4f$-$4d$ transitions from a number of ionization stages of tin, ranging from 8+ to 11+. The $5p$-$4d$ transitions of these ions and the 7+ ion form unresolved transition arrays (UTAs) in the wavelength range from 14 up to 23 nm. These UTAs are identified in Fig. 9. The wavelength ranges for each of the $5p$-$4d$ UTAs from 7+ to 10+ are listed in Table I. The features at lower wavelengths (below 12 nm) are believed to be caused by transitions to the $4d$ ground state configuration from higher energy levels $(5f,6p)$ of the same ions.

The fact that the $5p$-$4d$ emission features are separated in wavelength for the different ionization stages of tin, makes them suitable for deriving information on the time dependency of the populations of the various ion stages. To this end, time-resolved EUV spectra have been recorded from 75 ns before until 125 ns after the pinch. They have been integrated over three separate spatial regions in the plasma: close to the cathode (from 0.1 up to 0.45 mm from the cathode surface), further away from the cathode (from 1.15 to 1.5 mm away) and near the anode (3.0 to 3.35 mm from the cathode surface). For each ionization stage, the emission in a spectrum has been integrated over the corresponding wavelength range as given in Table I. For the near-cathode region, the integrated intensities have been plotted versus time in Fig. 10. Since the figure shows that the absolute emission from the 7+ and 8+ stages is much lower than the emission from the 9+ and 10+ ions, the curves have been replotted in Fig. 11, in which each curve has been normalized to its peak value.

TABLE I. The wavelength ranges that were used for integration of the radiation from the $5p$-$4d$ unresolved transition arrays (UTAs) of tin ionization stages from 7+ to 10+.

Ioniz. stage	λ_{min} (nm)	λ_{max} (nm)
7+	22.2	22.8
8+	19.5	20.1
9+	17.3	18.1
10+	15.5	16.3

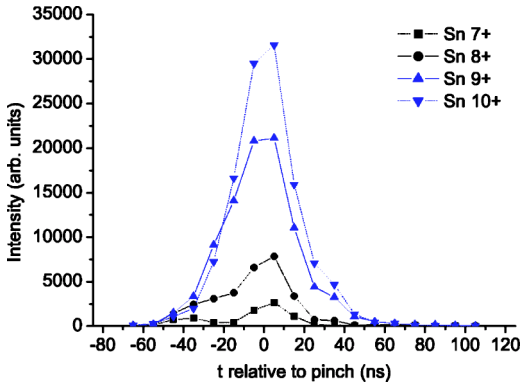

FIG. 10. Relative intensities of the $5p$-$4d$ UTAs of various tin ionization stages as a function of time during the pulse, as measured near the surface of the cathode.

Figure 11 shows that from 65 to 15 ns before the discharge, the spectrum tends toward increasing ionization stages. The emission from the 7+ ion even decreases after 35 ns before the pinch as it probably gets ionized further to higher stages. During this time, the plasma is heated by the strong electric current. However, during the pinch (around 0 ns on the time scale) the average ionization stage does not seem to increase further. The emission from the 10+ ion still increases somewhat relative to the Sn^{9+} emission; but on the

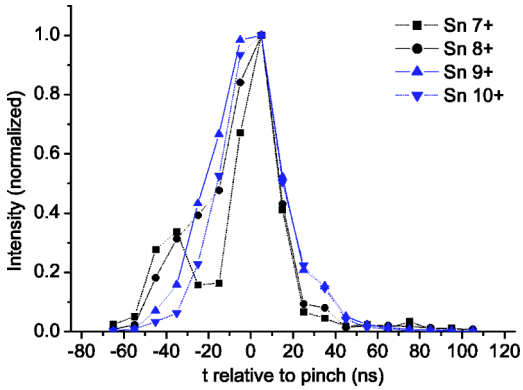

FIG. 11. $5p$-$4d$ UTA intensities measured near the cathode surface. Each curve is normalized to its own peak intensity during the discharge.

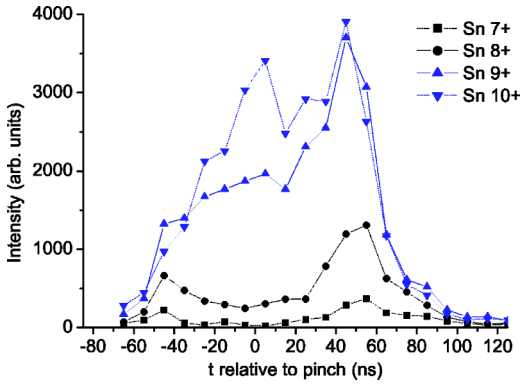

FIG. 12. Relative 5*p*-4*d* UTA intensities measured further away from the cathode surface.

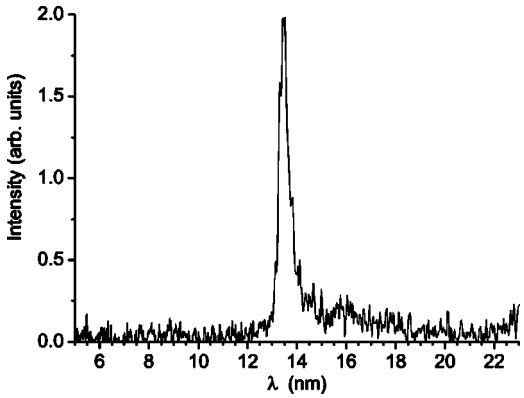

FIG. 13. The EUV spectrum as emitted by the plasma near the anode, 35 ns before the pinch.

other side, the relative importance of the 7+ and 8+ ion emission also increases. The plasma seems to be cooler than before the pinch. Perhaps cooler material near the discharge axis is mixed with hotter plasma from further away from the axis during the compression process. Additionally, the 9+ and 10+ radiation might be relatively more limited by opacity of the plasma, although it is still much weaker than the emission in the 4*f*-4*d* peaks at the same time.

Under the conditions that govern EUV discharges, with electron temperatures of a few tens of eV and electron densities up to about 10^{25} m^{-3}, the main recombination process is radiative recombination. For example, in the model of Colombant and Tonon [7], the contribution of three-particle recombination is less than 2% relative to the radiative recombination for the 9+ to 10+ ionization step, and taking plasma parameters T_e=35 eV and $n_e=1\times10^{25}$ m^{-3} that are typical for pinch plasmas. This means that the average ion charge will hardly decrease with increasing electron density, so that the increasing density due to the pinch effect can be excluded as the direct cause of the shift to lower ionization stages.

The EUV emission from the region further away from the cathode is much weaker than the emission from near the cathode, as is indicated by the intensity scale in Fig. 12. The same measurements were used as for Fig. 10 and the same procedure was followed. The figure shows that during the pinch, the emission from lower ionization stages in this region is relatively less important than in the near-cathode region, which is an indication of a hotter plasma. The EUV emission from this region has a longer duration than near the cathode. In this figure, a strong peak in the emission from the lower ionization stages appears about 50 ns after the pinch near the cathode. From the EUV pinhole images in Fig. 8, we know that this peak is probably caused by a volume of plasma that is moving in the upward axial direction away from the pinch. From the time delay between the appearance of the peak in the two regions, we can derive a velocity of the plasma of around 2×10^4 m s^{-1}. This velocity is about a factor two lower than the one derived in the previous section. However, such a difference can easily be explained by inaccuracies in the experiments and changes over time in the detailed behavior of the discharge.

Near the anode, the emission was even weaker and therefore too noisy to derive reliable time-dependent data in the manner described above. The EUV emission from this region is strongly peaked in time around 35 ns before the pinch, and consists almost exclusively of a peak in the spectrum near 13.5 nm, as is shown in Fig. 13. This behavior confirms that the emission near the anode is generated by a thin, but very hot plasma, as was already suggested in Sec. III.

V. CONCLUSIONS

The time-resolved visible and EUV images of the tin discharge plasma show a plasma that is created by the discharge current, and compresses to form a short-lived pinch on the axis of the source. After the pinch, a certain volume of plasma moves along the axial direction away from the cathode. The EUV spectra suggest that the ionization of the plasma takes place mainly before and during the compression of the plasma, and that the highest temperature is reached before the actual plasma pinch. These features all show strong qualitative similarities of the tin discharge with other EUV producing discharge plasmas, in particular the hollow cathode discharge.

However, a remarkable difference with the characteristics of the hollow cathode discharge is the sudden increase of the emission from relatively low ionization stages (7+, 8+ in the case of the tin discharge) during the pinch phase. Also for the hollow cathode discharge it was noticed that the average ionization degree seemed to be already slightly decreasing before the end of the compression phase [1], but the effect appears to be much stronger in the case of the tin discharge.

The spectra in the EUV range of the near-cathode region of the discharge confirm the suitability of the source for efficient production of EUV for application in lithography. The relative contribution of the region near 13.5 nm to the total spectrum is much larger than in the case of xenon plasmas.

Although some long-term changes in the behavior of the source cannot be excluded, the stability and reproducibility of the source on the short term were found to be good enough to perform more elaborate time-resolved experiments in which integration over a large numbers of pulses may be necessary. One technique that will require such experiments is Thomson scattering, a laser spectroscopic technique in which the spectrum of light from a laser pulse, scattered by

free electrons in the plasma, is recorded. On the basis of our findings, initial measurements using this technique have been performed, and the results of these have in the meantime been published as a different article [8].

[1] E. R. Kieft, J. J. A. M. van der Mullen, G. M. W. Kroesen, and V. Banine, Phys. Rev. E **68**, 056403 (2003).

[2] Proceedings of the EUV Source Workshop, International SEMATECH, Antwerp, Belgium, 2003, edited by V. Bakshi (unpublished).

[3] R. D. Cowan, *The Theory of Atomic Structure and Spectra* (University of California Press, Berkeley, 1981) (code in a version for personal computers, edited by A. Kramida, at http://das101.isan.troitsk.ru/cowan.htm).

[4] R. L. Kelly, Kelly Atomic Line Database, accesssible through http://cfa-www.harvard.edu/amdata/ampdata/kelly/kelly.html.

[5] G. A. Johannesson, T. Lundstrom, and L. Minnhagen, Phys. Scr. **6**, 129 (1972).

[6] C. E. Moore, *Atomic Energy Levels: As Derived from the Analysis of Optical Spectra* (US National Bureau of Standards, Washington, D.C., 1971).

[7] D. Colombant and G. F. Tonon, J. Appl. Phys. **44**, 3524 (1973).

[8] E. R. Kieft, J. J. A. M. van der Mullen,G. M. W. Kroesen, V. Banine, and K. N. Koshelev, Phys. Rev. E **70**, 056413 (2004).